

Temperature Determination by Means of Optoacoustic Measurements

John Gorman¹, Eph Sparrow¹, & John Abraham²

¹Department of Mechanical Engineering, University of Minnesota, Minneapolis, MN, USA

²School of Engineering, University of St. Thomas, St. Paul, MN, USA

Correspondence: Dr. John Abraham, University of St. Thomas, School of Engineering. E-mail: jpabraham@stthomas.edu

Received: April 30, 2014 Accepted: May 19, 2014 Available online: May 22, 2014

doi:10.11114/set.v1i2.420

URL: <http://dx.doi.org/10.11114/set.v1i2.420>

Abstract

The capabilities of the optoacoustic principle as a means of temperature measurement have been explored by means of experiments. In the experiments, a tissue test specimen, biological muscle sample, was positioned in a precisely temperature-controlled environment and irradiated with 532-nm laser light. The absorbed radiation gave rise to thermal expansion whose induced stresses created a sound field which was detected by a piezoelectric sensor. During the course of the experiments, the temperature of the water bath was systematically varied, with ample time being allowed to enable the test specimen to achieve thermal equilibrium. The temperature variation encompassed both increasing and decreasing protocols. Replicate samples were tested to ensure accuracy. It was found that temperature increases gave rise to decreasing acoustic amplitudes. An opposite trend was observed when the temperature was decreased. This outcome, when compared with the published literature, suggested that accurate use of the photoacoustic effect as a means of temperature measurement requires great care in the setup and execution of the experiment.

Keywords: optoacoustics, temperature measurement, chicken muscle, thermal measurements, thermal stress

1. Introduction

A novel means of noninvasive temperature measurement is based on an optoacoustic phenomenon. If a solid medium or radiation-absorbing liquid is irradiated by a pulsed laser, the absorbed energy gives rise to a very rapid thermal expansion. That expansion may produce a detectable acoustic wave. For the specific medium in question, the amplitude of the acoustic wave can be correlated with the temperature of the medium. The absorbed laser energy is too small to bring about significant temperature changes, so that the temperature of the medium is controlled by that of its immediate surroundings. A representative sample of the relevant literature is conveyed in (Esenaliev et al., 2000; Larin et al., 2005; Nikitin et al., 2012a; Nikitin et al., 2012b; Petrova et al., 2013; Shah et al., 2009; Pramanik & Wang, 2009).

Among these studies, a number of significant differences in instrumentation, laser wavelength, irradiated medium, and acoustic results was encountered. In (Nikitin et al., 2012a; Nikitin et al., 2012b), a 1064-nm laser beam was rotated by 90° to enable the sound-detecting piezoelectric transducer to be positioned upstream of the irradiated specimen. The specimens, all biological, were positioned in a heated water bath. For two of the specimens, chicken breast muscle and porcine liver, the acoustic amplitude increased with increasing temperature and decreased as the specimen was cooled. On the other hand, the opposite trends were observed for porcine lard. In contrast, in (Larin et al., 2005) heating was accomplished by conductive contact with a heated plate. The test specimen was canine liver, and the acoustic signal, produced from a 355-nm laser beam, also increased with increasing temperature. However, the positioning of the piezoelectric sensor differed for the two aforementioned experiments, either upstream (Nikitin et al., 2012a; Nikitin et al., 2012b) or downstream of the test specimen (Larin et al., 2005).

Significantly different specimens have been used by other investigators (Shah et al., 2009), including mineral oil, ink in water, water, and turkey in saline. Only cooling experiments were performed that yielded an acoustic amplitude, based on irradiation at 532-nm, which tended to decrease with decreasing temperature. In these experiments, the piezoelectric transducer was situated at the side of the specimen. The same wavelength of radiation and the same side positioning of the transducer was adopted in a study (Pramanik and Wang, 2009) which used a pair of laser-beam-impinged samples, including polyvinyl alcohol phantoms (with and without gold nanoparticles) and porcine muscle with injected gold nanoparticles immersed in water. The experiments were confined to heating over a small temperature range. No effect

of the presence of the nanoparticles was observed, and the acoustic signal increased with increasing temperature.

The Grüneisen parameter Γ (Grüneisen, 1926) is one of the key material properties contributing to optoacoustic phenomena. It is defined as

$$\Gamma = \frac{\beta c^2}{c_p} \quad (1)$$

where β is the volumetric coefficient of thermal expansion, c is the velocity of sound, and c_p is the constant pressure specific heat. It is well established that the Grüneisen parameter is extremely difficult to be measured as a single entity, so that its value has to be determined from its constituents. The variation of Γ with temperature controls the direction of change of the acoustic amplitude in response to temperature increases and decreases.

Values of Γ differ widely for biological media and may be contradictory for the same medium. For instance, for water and aqueous solutions, $\Gamma = 0.1$ at room temperature, and for fat, lipids, and oil, $\Gamma = 12.7$ (Castelino, et al., 2008). On the other hand, according to (Cox et al., 2009), Γ for fat is 0.7-0.9 and has a value of 0.25 for blood. In addition, Γ is likely to vary spatially throughout the medium (Cox et al., 2009).

The present investigation was undertaken to clarify the relationship between the temperature of a medium and the amplitude of the acoustic waves produced by impinging laser radiation. In this regard, the temperature of the medium is controlled by that of the surroundings in which it is situated. It will be demonstrated that the relationship between temperature and the optoacoustic amplitude is by no means as universal as might be expected on the basis of literature information.

The equipment which constitutes the experimental setup is displayed in Figure 1. The components of the setup will be described by following the path of the light emitted by a laser as it passes through the system. A Nd:YAG laser (Surelite I-10 Continuum, frequency = 10 Hz, pulse width = 6 ns, beam diameter = 4 mm, pulse energy ~ 5 mJ) produces optical radiation having a wavelength of 532 nm (green light). The heart of the apparatus is the test section which is an open-topped, glass-walled, five-gallon water bath and the constituents that it contains. The overall dimensions of the bath were 45 × 20 × 30 cm (length × width × height). Prior to its use, the internal and external surfaces of the glass walls were physically and chemically cleansed. The water itself had been degassed before use and subsequently stored in inert-walled containers.

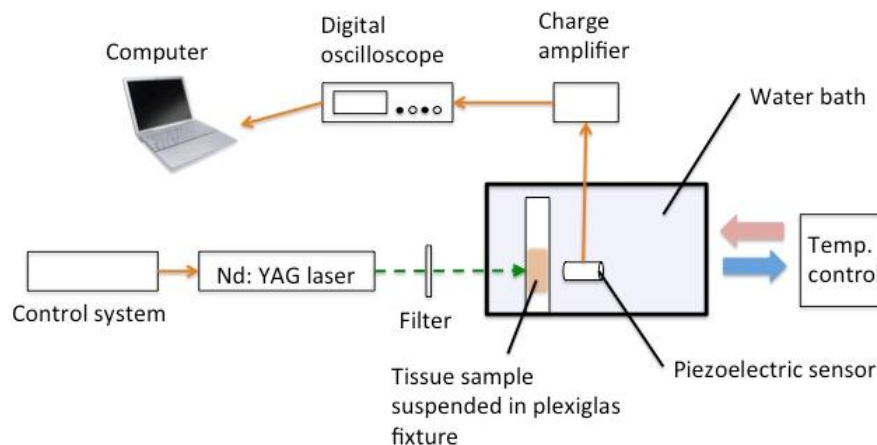


Figure 1. Schematic diagram of the experimental setup.

The water bath housed two major components. One of these is a specially designed and fabricated tissue housing made from plexiglass. An exploded view of the housing is displayed in Figure 2. As can be seen from the figure, the housing consists of three rectangular plates of plexiglass having equal face dimensions. These plates are assembled in the form of a sandwich. The forward-facing plate of the sandwich is seen to have a square aperture cut into its exposed face. There is an identical aperture cut into the rearward-facing plate. The middle plate of the sandwich houses the test specimen by means of an aperture cut precisely to accommodate it. The specimen is held loosely in place by frictional interaction with the front and back plates of the sandwich. The open apertures expose the test specimen to the water environment.

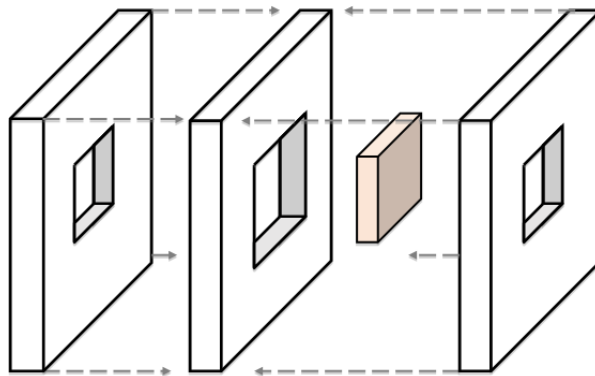


Figure 2. Housing of the test sample.

Figure 3 is a photograph of the experimental arrangement. As seen in the figure, a piezoelectric sensor (10 MHz Olympus immersion transducer A311S-SU) is located directly behind the test specimen in the water bath. The sensor detects the amplitude of pressure waves emitted from the sample as a function of time. The electronic signal from the sensor is conveyed to an amplifier (Panametrics 5072PR) and then to a digital oscilloscope (LeCroy WaveJet 354).

The final component of the experimental-setup schematic of Fig. 1 is a thermostatically controlled, pump-equipped water reservoir. The control function is able to maintain the water temperature to within 0.1 °C. This reservoir and the bath continuously interchange temperature-controlled water.

Fresh (never frozen) chicken breast muscle was used as the tissue sample. It was cut to size: 1 × 5 × 5 cm (thickness × height × width). Prior to its use, the sample was degassed under vacuum and subsequently sealed in an airtight container.

Prior to the initiation of the experiments, all water bath components were at a uniform temperature, and at the moment of the initiation, the thermostatic source provided water to the bath at the same temperature. The adopted experimental protocol enabled a continuously increasing water temperature to be delivered to the water bath. Water bath temperatures were recorded at 2 °C intervals (after an equilibration period of about 6.6 minutes) along with simultaneous recording of the output of the piezoelectric sensor.

To provide confirmation of the trends in the data, three totally independent experiments were performed. For each such experiment, a fresh muscle sample was employed. The results of the replicate experiments were indistinguishable from each other.

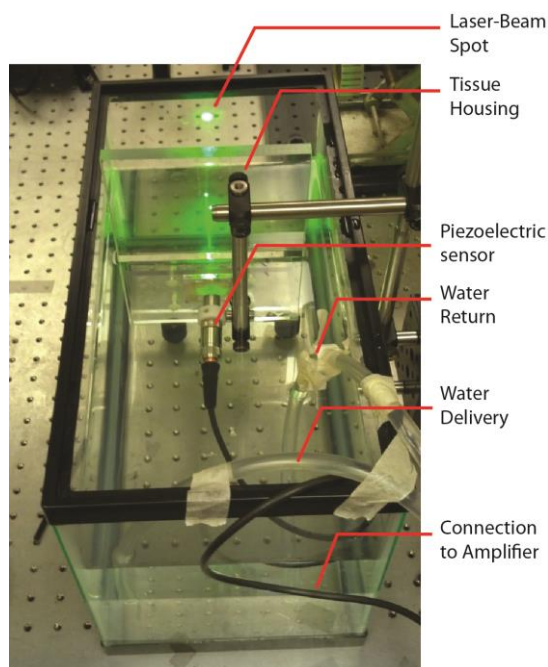


Figure 3. Photograph of the experimental arrangement.

2. Results and Discussion

To exemplify the nature of the collected experimental information, Figure 4 has been prepared. The figure, taken from the output of an oscilloscope, shows the sound wave amplitude at a particular moment of time which corresponds to the simultaneous reading of the bath temperature.

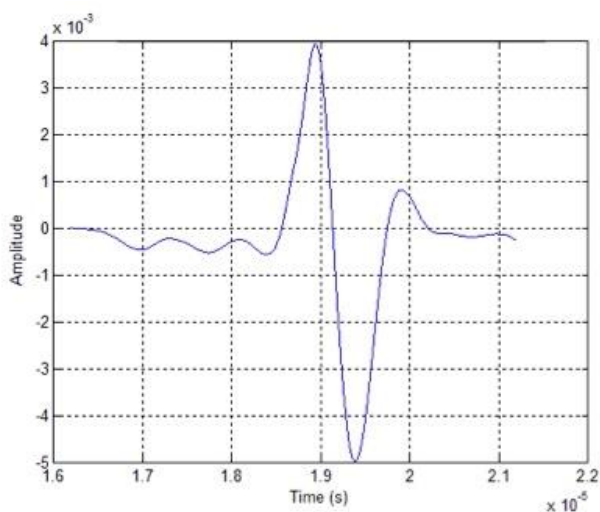


Figure 4. Typical trace of sound-wave amplitude in volts from the oscilloscope output.

Peak-to-valley values were extracted from the collected data and were post-processed to yield the amplitude of the signal. This information was paired with the temperature data collected at the same instant of time. A graph showing the variation of the sound-wave amplitude as a function of temperature is presented in Figure 5. The figure includes results for both heating and cooling of the same chicken muscle sample. The information displayed in this figure was reproduced with the results of the replicate experiments.

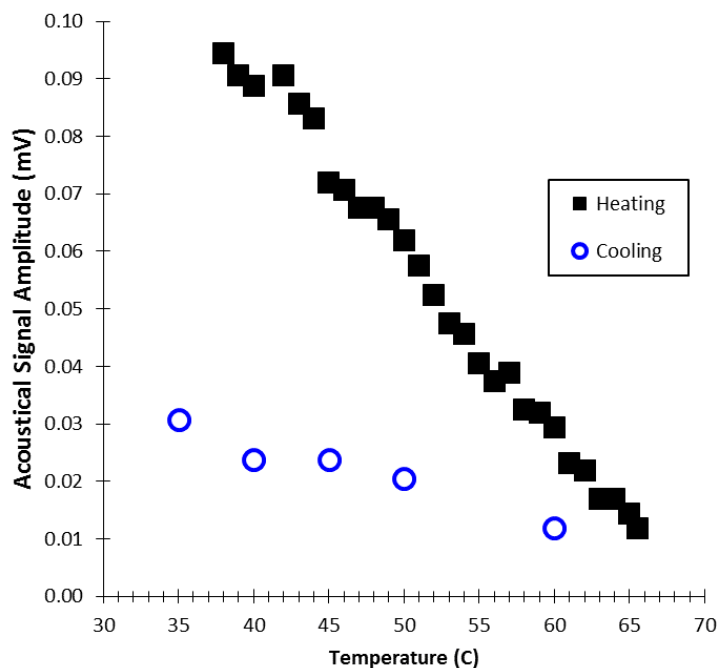


Figure 5. Variation of the sound-wave amplitude with temperature.

Inspection of the figure reveals a strong trend in which the amplitude of the sound wave decreases monotonically with increasing sample temperature. With respect to cooling, it is worthy of note that those experiments followed directly after the heating data were obtained, so that the material properties of the tissue during the cooling experiments were

different from those during the heating experiments. This change of properties is responsible for the cooling results to follow a path different from that displayed by the heating results.

As is well established (Murphy and Marks, 2000) chicken breast muscle undergoes significant changes as its temperature increases. Heating produces a softening of connective tissue caused by conversion of collagen to gelatin. Also, there are significant changes in texture as a result of the aforementioned changes in the connective tissue fiber and in the muscle fibers as well. Heat-induced changes in protein solubility give rise to changes in the water-capacity of the tissue. These processes clearly support the notion that there is a continuous change in the material properties of the muscle during heating.

A quantitative estimate of the extent of the laser beam penetration for raw hydrated muscle can be obtained from the formula (Ritz et al., 2001):

$$\text{Depth of penetration} = [3\mu_a(\mu_a + \mu_s(1 - g))]^{-1/2} \quad (2)$$

where μ_a and μ_s respectively represent the absorption and scattering coefficients in units of cm^{-1} . The quantity g is the anisotropic factor. Numerical values for a wavelength of 550 nm are $\mu_a = 0.6 \text{ cm}^{-1}$, $\mu_s = 3.4 \text{ cm}^{-1}$, and $g = 0.8$ (Firdous et al., 2005). Evaluation of Eq. (2) results in a depth of penetration 0.66 cm. Inasmuch as the sample thickness used in the present experiments is 1 cm, only part of the sample was penetrated.

It is relevant to make a trendwise comparison of the present results with representative results from the published literature. In (Nikitin, et al., 2012a), results of the type presented in Figure 5 were presented both for chicken breast muscle and for porcine lard, whereas in (Wang & Emelianov, 2011) similar information was conveyed for lipids in plaque and in fatty tissue. These results displayed a variety of trends. The chicken-breast muscle results of (Nikitin, et al., 2012a) showed trends opposite to those found here, as did the lipids-in-plaque results of (Wang & Emelianov, 2011). On the other hand, the porcine-lard (Nikitin, et al., 2012a) and the fatty-tissue (Wang & Emelianov, 2011) results exhibited trends that agreed with those observed here.

There are several factors to which the different trends for chicken breast muscle between the present results and those of (Nikitin, et al., 2012a) can be attributed. One of these is the manner in which the muscle specimen was housed. In (Nikitin, et al., 2012a), it appears that the specimen was heavily loaded from above, so that the specimen might have undergone forced contraction as the internal changes described earlier took place. It is likely that the naturally occurring structural changes might have been inhibited. Another factor relates to the optical properties in the presence of different irradiating radiation. In the present experiments, the laser provided radiation at a wavelength of 532 nm (green light) whereas the participating radiation in (Nikitin, et al., 2012a) corresponded to a wavelength 1064 nm (IR). It has been noted (Esenaliev et al., 2002) that, in general, absorption is low and scattering is significantly reduced in tissue for radiation in the wavelength range between 600 and 1300 nm. Still another issue to which the trendwise differences can be attributed is the different placement of the piezoelectric sensor. In the present experimental setup, the sensor was situated in the water bath immediately behind the specimen under investigation. On the other hand, in (Nikitin, et al., 2012a), the sensor was positioned in front of the sample and outside of the water bath.

The issue of the sensor location can be made physically plausible. It can be reasoned that the temperature gradients in the forward-facing portion of the tissue will be larger than those in the rearward-facing portion. The underlying reason for this occurrence is that photon absorption depletes the intensity of the radiation beam so that the rate of absorption necessarily decreases in the beam direction. The depletion is abetted by any backward scattering that occurs. Diminished gradients correspond to lesser thermal expansion and, consequently, to diminished sound-wave production. These effects are accentuated as the tissue properties are altered as heating proceeds.

3. Conclusion

Careful experiments were performed to enrich the knowledge base relevant to the use of the photoacoustic effect for temperature measurements. Special care was given to the establishment of the temperature of the specimen used in the experiments. A thermostatically controlled, well-stirred water bath was employed as the test environment. The piezoelectric sensor was positioned in the water bath contiguous to the specimen in order to avoid possible interference between the creation of the acoustic signal and its measurement.

It was found that the amplitude of the acoustic signal decreased with increasing temperature and increased when the temperature of the specimen decreased. This outcome was not in synch with that of an earlier study. It was conjectured that the different trends might well have been caused by the different conditions under which the experiments were performed. It may be concluded that the photoacoustic effect can be a viable means of temperature measurement provided that the experiments are carefully configured. In the case of biomedical tissue, it is essential that the means of housing the specimen do not constrain the physiological changes that naturally occur as the temperature of

the specimen is varied.

References

- Castelino, R., Whelan, W. M., & Kolios, M. C. (2008). Photoacoustic detection of protein coagulation in albumen-based phantoms. *Proc. SPIE*, 6856, March 12, San Jose, CA, paper no. 685626-1. <http://dx.doi.org/10.1117/12.764305>
- Cox, B. T., Laufer, J. G., & Beard, P. C., (2009). The challenges for quantitative photoacoustic imaging. *SPIE BiOS: Bio. Opt. International Society for Optics and Photonics*, January 24-29, San Jose, CA, paper no. 717713, <http://dx.doi.org/10.1117/12.806788>
- Esenaliev, R. O., Larina, I. V., Larin, K. V., Deyo, D. J., & Motamedi, M. (2000). Real-time optoacoustic monitoring during thermotherapy. *Bio. Optoacoustics, Proc. SPIE* 3916, May 19, San Jose, CA, 302-310. <http://dx.doi.org/10.1117/12.386334>
- Esenaliev, R. O., Larina, I. V., Larin, K. V., Deyo, D. J., Motamedi, M., & Prough, D. S. (2002). Optoacoustic technique for noninvasive monitoring of blood oxygenation: a feasibility study. *Appl. Opt.*, 41(22), 4722-4731, <http://dx.doi.org/10.1364/AO.41.004722>
- Firdous, S., Ikram, M., Nawaz, M., & Aslam, M. (2005). Measurement of an optical parameters: absorption scattering and auto-florescence of skin in vitro. *Int. J. Cancer Res.*, 1(1-2), 10-15. <http://dx.doi.org/10.3923/ijcr.2005/.10.15>.
- Grüneisen, E. *Handbuch der Physik*, Springer, Berlin. (1926).
- Larin, K. V., Larina, I. V., & Esenaliev, R. O. (2005). Monitoring of tissue coagulation during thermotherapy using optoacoustic technique. *J. Phys. D: Appl. Phys.*, 38(15), 2645. <http://dx.doi.org/10.1088/0022-3727/38/15/017>
- Murphy, R., & Marks, B. P. (2000). Effect of meat temperature on proteins, texture, and cook loss for ground chicken breast patties. *Poultry Sci.*, 79(1), 99-104.
- Nikitin, S. M., Khokhlova, T. D., & Pelivanov, I. M. (2012a). Temperature dependence of the optoacoustic transformation efficiency in ex vivo tissues for application in monitoring thermal therapies. *J. Bio. Opt.*, 17(6), 0612141-0612149. <http://dx.doi.org/10.1117/1.JBO.17.6.061214>
- Nikitin, S. M., Khokhlova, T. D., & Pelivanov, I. M. (2012b). In-vitro study of the temperature dependence of the optoacoustic conversion efficiency in biological tissues. *Quant. Electronics*, 42(3), 269. <http://dx.doi.org/10.1070/QE2012v042n03ABEH014674>
- Petrova, E., Ermilov, S., Su, S., Nadvoretzkiy, V., Conjusteau, A., & Oraevsky, A. (2013). Using optoacoustic imaging for measuring the temperature dependence of Grüneisen parameter in optically absorbing solutions. *Opt. Express*, 21(21), 25077-25090. <http://dx.doi.org/10.1364/OE.21.025077>
- Pramanik M., & Wang, L. V. (2009). Thermoacoustic and photoacoustic sensing of temperature. *J. Bio. Opt.*, 14(5), 054024. <http://dx.doi.org/10.1117/1.3247155>
- Ritz, J.-P., Roggan, A. Isbert, C., Müller, G. Buhr, H., & Germer, C.-T. (2001). Optical properties of native and coagulated porcine liver tissue between 400 and 2400 nm. *Lasers Surg. Med.*, 29(3), 205-212.
- Shah, J., Park, S. Aglyamov, S., Larson, T., Ma, L., Sokolov, K., Johnston, K., Milner, T., & Emelianov, S. Y. (2009). Photoacoustic imaging and temperature measurement for photothermal cancer therapy. *J. Bio. Opt.*, 13(3), paper no. 034024. <http://dx.doi.org/10.1117/1.294036>
- Wang B., & Emelianov, S. (2011). Thermal intravascular photoacoustic imaging. *Bio. Opt. Express*, 2, 3072–3078. <http://dx.doi.org/10.1364/BOE.2.003072>



This work is licensed under a [Creative Commons Attribution 3.0 License](https://creativecommons.org/licenses/by/3.0/).